ApJ Letters, submitted, September 14, 2016
Preprint typeset using LaTeX style emulateapj v. 5/2/11

FIRST GAIA LOCAL GROUP DYNAMICS: MAGELLANIC CLOUDS PROPER MOTION AND ROTATION

Roeland P. van der Marel
Space Telescope Science Institute, 3700 San Martin Drive, Baltimore, MD 21218

Johannes Sahlmann
European Space Agency, Space Telescope Science Institute, 3700 San Martin Drive, Baltimore, MD 21218, USA
ApJ Letters, submitted, September 14, 2016

ABSTRACT

We use the *Gaia* data release 1 (DR1) to study the proper motion (PM) fields of the Large and Small Magellanic Clouds (LMC, SMC). This uses the *Tycho-Gaia* Astrometric Solution (TGAS) PMs for 29 *Hipparcos* stars in the LMC and 8 in the SMC. The LMC PM in the West and North directions is inferred to be $(\mu_W, \mu_N) = (-1.874 \pm 0.039, 0.223 \pm 0.049)$ mas yr^{-1} , and the SMC PM $(\mu_W, \mu_N) = (-0.876 \pm 0.060, -1.227 \pm 0.042)$ mas yr^{-1} . These results have similar accuracy and agree to within the uncertainties with existing Hubble Space Telescope (*HST*) PM measurements. Since TGAS uses different methods with different systematics, this provides an external validation of both data sets and their underlying approaches. Residual DR1 systematics may affect the TGAS results, but the *HST* agreement implies this must be below the random errors. Also in agreement with prior *HST* studies, the TGAS LMC PM field clearly shows the clockwise rotation of the disk, even though it takes the LMC disk in excess of 10^8 years to complete one revolution. The implied rotation curve amplitude for young LMC stars is consistent with that inferred from line-of-sight (LOS) velocity measurements. Comparison of the PM and LOS rotation curves implies a kinematic LMC distance modulus $m - M = 18.53 \pm 0.42$, consistent but not yet competitive with photometric methods. These first results from *Gaia* on the topic of Local Group (LG) dynamics provide an indication of how its future data releases will revolutionize this field.

Subject headings: proper motions — galaxies: individual (Large Magellanic Cloud, Small Magellanic Cloud) — galaxies: kinematics and dynamics — Magellanic Clouds

1. INTRODUCTION

Almost everything that is known about LG dynamics, and of galaxy dynamics in general, is based on LOS velocity observations. Such measurements constrain only one component of motion, and interpretation therefore requires that various assumptions be made. PMs in the plane of the sky provide a more complete picture. However, the PMs are generally small and inversely proportional to the distance of the target.

The *Hipparcos* satellite provided a detailed understanding of the PMs of stars in the solar neighborhood (ESA 1997), but its accuracy was insufficient for detailed studies of other LG objects. Water maser observations yielded the first accurate PMs for other LG galaxies (Brunthaler et al. 2005). However, this technique is limited to the few LG objects with high star formation rates. Only with *HST* has it become possible to determine PMs for objects throughout the LG. For example, the HSTPROMO collaboration has studied the PM dynamics of globular clusters, stellar streams, and nearby galaxies (van der Marel 2015).

The *Gaia* satellite will provide the next step forward through PM measurements for objects across the sky to magnitude $\sim$ 20 (Gaia Collaboration 2016a). Initial five-parameter astrometric solutions (including PMs) are expected in late 2017, with a final DR in 2022. By contrast, the *Gaia* DR1 of Sep 14, 2016, includes PMs only for stars in common between *Gaia* and the *Hipparcos* Tycho-2 Catalogue (Gaia Collaboration et al. 2016b; Lindegren et al. 2016). This Tycho-*Gaia* Astrometric Solution (TGAS) Catalog is restricted to the same bright stars previously studied by *Hipparcos* and is therefore not well suited for studies of LG dynamics. However, we show in this paper that it does yield some first new insights.

The LMC and SMC are the most massive satellites of the Milky Way (MW). They have been studied extensively to improve our understanding of a wide range of astrophysical subjects. To place these results in a proper context, it is important to understand the dynamics of the Magellanic Clouds (MCs) and their history in the LG. They have therefore been of special interest for *HST* studies. Kallivayalil et al. (2006a,b) presented PMs for 26 fields based on two epochs of *HST* data with a 2-year time baseline. These measurements were refined by Kallivayalil et al. (2013; hereafter K13) using a third epoch for 12 fields, which extended the time baseline to 7 years. The latter provided a median per-coordinate PM uncertainty of only 0.03 mas/yr (7 km/s), 3–4 times better than the two-epoch measurements.

The *HST* studies showed that the MCs move faster about the MW than previously believed based on models of the Magellanic Stream. So instead of being long-term satellites, they are most likely on their first MW passage (Besla et al. 2007). These results have refined our understanding of the MCs, as well as the formation of Magellanic Irregulars in general (Besla et al. 2012). van der Marel & Kallivayalil (2014; hereafter vdMK14) studied the variations in the *HST* PM measurements across the face of the LMC. They measured the PM rotation

Table 1
TGAS Proper Motions of Magellanic Cloud stars

HIP ID	*Gaia* sourceId	RA (deg)	dec (deg)	PM_W (mas/yr)	PM_N (mas/yr)
LMC					
22392	4655349652394811136	72.3017	-69.4565	-2.012 ± 0.151	-0.226 ± 0.151
22758	4655510043652327552	73.4304	-68.7148	-1.772 ± 0.160	-0.296 ± 0.171
22794	4655460771785226880	73.5594	-69.2101	-1.895 ± 0.088	-0.122 ± 0.088
22849	4661769941306044416	73.7390	-66.7524	-1.756 ± 0.120	-0.045 ± 0.130
22885	4661720532007512320	73.8400	-67.4365	-1.766 ± 0.145	-0.030 ± 0.147
22900	4655136518933846784	73.8853	-69.9625	-1.951 ± 0.232	-0.102 ± 0.221
22989	4655158131209278464	74.1962	-69.8402	-1.869 ± 0.234	0.015 ± 0.227
23177	4662293892954562048	74.7878	-65.6677	-1.613 ± 0.162	0.026 ± 0.159
23428	4654621500815442816	75.5308	-71.3370	-1.973 ± 0.146	-0.099 ± 0.140
23527	4655036841335115392	75.8733	-70.6998	-1.942 ± 0.240	0.077 ± 0.230
23665	4661920986713556352	76.3009	-66.7368	-1.675 ± 0.104	0.005 ± 0.114
23718	4661472145451256576	76.4813	-67.8864	-1.785 ± 0.072	0.123 ± 0.079
23820	4662061311885050624	76.8091	-66.0551	-1.555 ± 0.212	0.238 ± 0.216
24006	4651629489160555392	77.4122	-71.4006	-2.236 ± 0.105	0.065 ± 0.098
24080	4658269336800428672	77.5950	-68.7733	-1.896 ± 0.092	0.169 ± 0.094
24347	4658204053297963392	78.3783	-69.5399	-2.084 ± 0.196	0.251 ± 0.177
24694	4658137739001073280	79.4433	-69.8492	-1.882 ± 0.131	0.182 ± 0.126
24988	4660601607121368704	80.2571	-65.8007	-1.499 ± 0.079	0.387 ± 0.089
25097	4660444926713007872	80.5878	-66.2603	-1.510 ± 0.173	0.337 ± 0.191
25448	4658486455992620416	81.6454	-68.8687	-1.710 ± 0.138	0.587 ± 0.133
25615	4660175580731856128	82.0847	-67.4051	-1.568 ± 0.204	0.479 ± 0.208
25892	4660124762671796096	82.9101	-67.4699	-1.587 ± 0.182	0.669 ± 0.186
26135	4660246224352015232	83.5936	-67.0232	-1.633 ± 0.095	0.429 ± 0.113
26222	4657280635327480832	83.8193	-69.6773	-1.723 ± 0.187	0.497 ± 0.188
26338	4657700408260606592	84.1349	-68.9005	-1.874 ± 0.185	0.621 ± 0.200
26745	4657627943562907520	85.2409	-69.2586	-1.779 ± 0.231	0.518 ± 0.242
27142	4657722879521554176	86.3193	-68.9978	-1.733 ± 0.142	0.705 ± 0.137
27819	4659188769038018816	88.2918	-68.1186	-1.560 ± 0.153	0.834 ± 0.106
27868	4659091084305723392	88.4571	-68.3132	-1.661 ± 0.154	0.843 ± 0.111
straight mean[1]				-1.776 ± 0.033	0.246 ± 0.059
weighted mean[2]				-1.773 ± 0.024	0.240 ± 0.025
SMC					
3934	4685876046561549184	12.6316	-73.4785	-0.541 ± 0.177	-1.304 ± 0.177
3945	4685876046561548800	12.6600	-73.4717	-0.668 ± 0.154	-1.160 ± 0.148
4004	4689033534707612800	12.8525	-72.3829	-0.670 ± 0.148	-1.165 ± 0.143
4126	4685940436697751168	13.2135	-73.1149	-0.667 ± 0.132	-1.291 ± 0.116
4153	4688967357860689024	13.2704	-72.6334	-0.821 ± 0.131	-1.231 ± 0.130
4768	4690499767820637312	15.3208	-72.2920	-1.144 ± 0.151	-1.239 ± 0.143
5267	4687436700227349888	16.8259	-72.4677	-0.849 ± 0.152	-1.262 ± 0.144
5714	4687159863816994816	18.3771	-73.3362	-0.992 ± 0.091	-1.182 ± 0.082
straight mean[1]				-0.794 ± 0.066	-1.229 ± 0.018
weighted mean[2]				-0.833 ± 0.047	-1.221 ± 0.045

Note. — Column (1)-(2): *Hipparcos* ID and *GAIA* sourceId number of those MC stars previously identified by Kroupa & Bastian (1997) and analyzed here. Columns (3)-(6): right ascension α, declination δ, proper motion $PM_{W(est)}$ ($\equiv -PM_\alpha \cos\delta$), and $PM_{N(orth)}$ ($\equiv PM_\delta$) from the TGAS catalog. All stars have known LOS velocities (Barbrier-Brossat et al. 1994; Kroupa & Bastian 1997; Neugent et al. 2012; Kordopatis et al. 2013) consistent with LMC or SMC membership. Only stars with TGAS `astrometric_excess_noise` ≤ 1.02 mas were retained, which rejects HIP 22237 and 25815 in the LMC. HIP 7912 and 8470 near the SMC were excluded because they reside in the Magellanic Bridge. HIP 23500, 24907, 25146, 25822, and 27655 in the LMC, and HIP 5397 in the SMC are not listed in the TGAS catalog. There are no additional *Hipparcos* stars with both position and kinematics (SIMBAD LOS velocity and TGAS PM) consistent with MC membership. The straight and weighted mean for each MC are listed, for simplicity not accounting for the covariances between the TGAS astrometric parameters.

[1] The uncertainty in the "straight" mean is based exclusively on the observed scatter, and doesn't use the individual PM uncertainties.

[2] The uncertainty in the weighted mean is based exclusively on the individual PM uncertainties, and doesn't use the observed scatter. This underestimates the PM uncertainty in the COM motion of each MC.

curve, and demonstrated consistency with LOS velocity studies.

Historically, one of the first measurements of the MC PMs was obtained by Kroupa & Bastian (1997), using data for 36 LMC stars and 11 SMC stars from the *Hipparcos* satellite. These are young massive stars with apparent V-magnitudes between 9–12 (absolute magnitudes brighter than −6.5). High-quality TGAS data exist for 29 of the LMC and 8 of the SMC stars. We retrieved these data from the *Gaia* archive using `pygacs`.[1] While the *Hipparcos* PM errors ranged from one to a few mas/yr, the errors for new TGAS PMs, listed in Table 1, are much smaller. The 0.15 mas/yr median error is similar to the *HST* PM errors for the K13 two-epoch fields. So while the TGAS measurements do not improve upon the *HST* measurements, they do allow for an independent verification. We therefore analyze here the MC

[1] `https://github.com/Johannes-Sahlmann/pygacs`

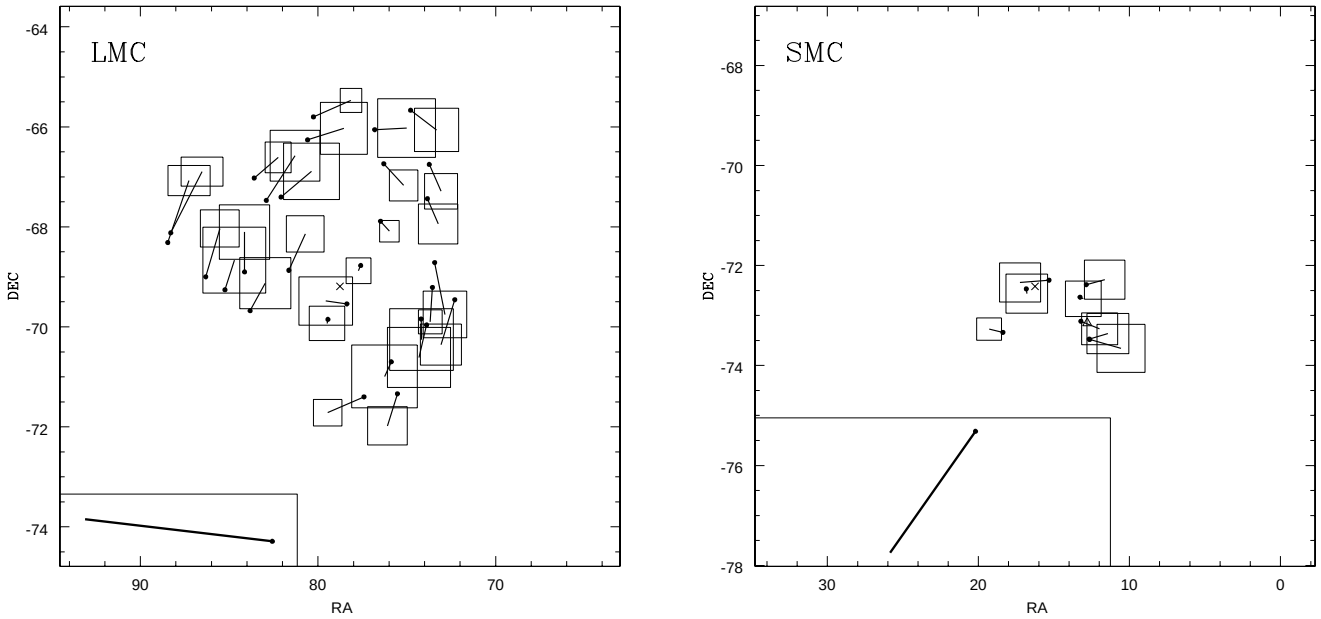

Figure 1. Spatially variable component of the observed TGAS PM fields for the LMC (left) and SMC (right), centered on the dynamical center (cross; a triangle for the LMC SMC indicates the photometric center of the old stars). The horizontal and vertical extent of each panel represent an equal number of degrees on the sky. Solid dots show the positions of the sample stars. The PM vector for each star is the observed PM from Table 1, minus the best-fit COM PM (shown in the inset on the bottom left; see column (3) of Tables 2 and 3). PM vectors have a size that indicates the mean predicted motion over (arbitrarily) the next 7.2 Myr. Open boxes at the end of the PM vectors approximate the 68.3% TGAS PM uncertainties. For the LMC, clockwise rotation is clearly evident.

TGAS PMs with the same methodologies presented in K13 and vdMK14. We do this for the LMC in Section 2, and the SMC in Section 3. Section 4 discusses the results in the context of previous work. Section 5 summarizes the conclusions.

2. LMC PROPER MOTION FIELD

Figure 1a shows the spatially variable component of the observed LMC PM field (comparable to Figure 1 of vdMK14 for the *HST* PM data). For each star in Table 1 we subtracted the best-fit LMC center-of-mass (COM) PM (figure inset) derived below. Clockwise motion is clearly evident. This qualitatively validates the accuracy of the data, and confirms that the stars belong to the LMC.

We model the LMC PM field to derive its kinematical and geometrical parameters. The model has contributions from the internal rotation of the LMC and the systemic motion of the LMC COM. To describe the former, we assume that the LMC is a flat disk with circular streamlines. The latter adds a spatially variable "perspective rotation" component (due to the fact that projection of the COM velocity vector onto the West and North directions depends on position). The relation between the transverse velocity v_t in km/s and the PM μ in mas/yr is given by $\mu = v_t/(4.7403885D)$, where D is the distance in kpc (since the LMC is an inclined disk, this distance D is not the same for all stars). We refer the reader to van der Marel et al. (2002; hereafter vdM02) for a derivation of full analytical expressions.

Table 2 lists the results of fitting this model to the data. Column (3) uses only the new TGAS PM data. The COM position is not well-constrained by the data, since there are very few TGAS stars on the south-east side of the LMC; we therefore keep it fixed at the value inferred by vdMK14. Column (4) includes also the *HST* PM data from vdMK14, which pertain to a mix of young and old stellar populations with apparent V-magnitudes between 16–24. This improves the constraints, but complicates the interpretation by mixing stars of different ages (which have different kinematics because of the phenomenon of asymmetric drift). Column (5) shows results obtained when the TGAS PMs are fit simultaneously with an age-matched sample of literature LOS velocities for 723 Red Supergiants (vdMK14).

These fits parameterize the rotation curve $V(R)$ as function of radius R in the disk to increase linearly to velocity V_0 at radius R_0, and then stay flat at larger radii. We also obtained a non-parametric estimate for $V(R)$ as in vdMK14, by determining for each star the PM component along the local direction of rotation. Green data points in Figure 2 show the rotation estimates thus obtained for the TGAS stars, while black data points show the results after binning in radius to decrease the error bars.

3. SMC PROPER MOTION FIELD

Figure 1b shows the spatially variable component of the observed SMC PM field, after subtraction of the best-fit COM PM (figure inset) derived below. The stars all have similar PMs, which confirms their SMC membership. No rotation in the plane of the sky is evident. This is due to two separate effects. First, the SMC is smaller than the LMC, and the TGAS stars are closer to the galaxy center then they are for the LMC. At small radii, both the intrinsic galaxy rotation and perspective rota-

Table 2
LMC Dynamical Model Parameters: Fit Results from Two- and Three-Dimensional Kinematics

Quantity	Unit	PMs TGAS	PMs TGAS+HST	PMs TGAS + Young Star $v_{\rm LOS}$
(1)	(2)	(3)	(4)	(5)
α_0	deg	78.76 ± 0.52[1]	78.80 ± 0.28	80.21 ± 0.40
δ_0	deg	-69.19 ± 0.25[1]	-69.17 ± 0.15	-69.25 ± 0.21
i	deg	44.1 ± 4.0	38.9 ± 3.2	30.2 ± 6.0
Θ	deg	123.6 ± 7.2	145.9 ± 6.5	153.7 ± 5.7
μ_{W0}	mas/yr	-1.874 ± 0.039	-1.903 ± 0.014	-1.854 ± 0.031
μ_{N0}	mas/yr	0.223 ± 0.049	0.235 ± 0.026	0.350 ± 0.035
$v_{\rm LOS,0}$	km/s	262.2 ± 3.4[1]	262.2 ± 3.4[1]	270.5 ± 3.3
V_0	km/s	108.4 ± 16.3	74.9 ± 5.7	77.8 ± 16.1
R_0	D_0	0.088 ± 0.014	0.027 ± 0.006	0.046 ± 0.005
D_0	kpc	50.1 ± 2.5 kpc[1]	50.1 ± 2.5 kpc[1]	50.8 ± 10.6 kpc

Note. — Columns (1)-(2): model quantity and units. Columns (3)-(5): values inferred from model fits described in Section 2. The listed quantities are: position (α_0, δ_0) of the dynamical center; inclination angle i and line-of-nodes position angle Θ of the disk plane; COM PM (μ_{W0}, μ_{N0}) and LOS velocity $v_{\rm LOS,0}$; rotation curve amplitude V_0 and turnover radius R_0; and distance D_0.

[1] (α_0, δ_0) from vdMK14; $v_{\rm LOS,0}$ from vdM02; D_0 based on distance modulus $m - M = 18.50 \pm 0.10$ from Freedman et al. (2001). Not fit, but uncertainty propagated into other model parameters.

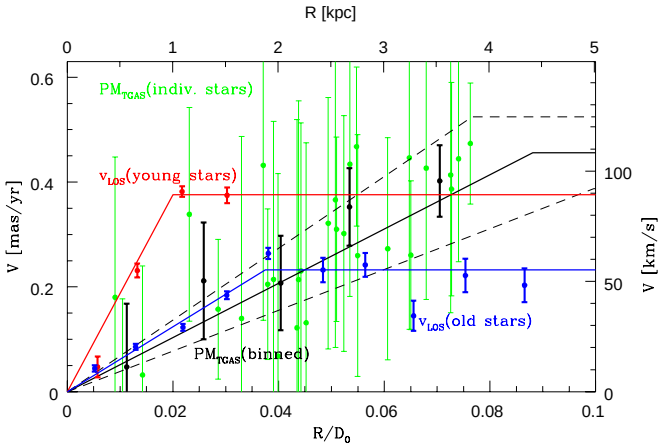

Figure 2. LMC disk rotation velocity V at cylindrical radius R. The left and bottom axes are expressed in angular and dimensionless units, while the right and top axes show physical units. Errorbars include only the random measurement noise, not propagated uncertainties from other LMC model parameters. Broken curves shows the best-fit parameterizations of the form used in Section 2. Red and blue data points show LOS rotation curves for samples of young and old stars (vdMK14). Green data points show the PM rotation curve inferred here from individual TGAS stars. Black data points show a radial binning of the TGAS results in 0.8 kpc bins, yielding 3, 2, 9, 8, and 7 stars in the subsequent bins, respectively. The binned data for $V(R)$, with V in km/s and R in kpc, are: $V(0.56) = 11.2 \pm 28.7$, $V(1.29) = 50.3 \pm 26.5$, $V(2.03) = 49.2 \pm 21.4$, $V(2.68) = 83.8 \pm 17.6$, and $V(3.53) = 95.5 \pm 16.2$.

tion components are smaller. Second, photometric and LOS velocity studies show that the SMC is more vertically extended and less rapidly rotating (if at all) than the LMC (van der Marel et al. 2009).

In view of these facts and the small number of stars, we fit a relatively simple model to the SMC PM field, as in K13. We include perspective rotation and allow for a single overall intrinsic galaxy rotation velocity $V_{\rm rot}$ in the plane of the sky (i.e., as though we were viewing a face-on disk). We keep the distance modulus fixed at $m - M = 18.99 \pm 0.10$ (Cioni et al. 2000b), and the radial velocity fixed at $v_{\rm sys} = 145.6 \pm 0.6$ km/s (Harris & Zaritsky 2006).

We explored several different fits, in which the SMC COM PM is always a free parameter. We keep the COM position fixed, since it is not well constrained by the PM data in absence of rotation. We use either the HI kinematical center from Stanimirovic et al. (2014), or the photometric center of the old stars from Cioni et al. (2000a), in each case with an uncertainty of 0.2° per coordinate. We treat $V_{\rm rot}$ either as a free parameter, or keep it fixed to $V_{\rm rot} = 0 \pm 40$ km s^{-1}. The assigned uncertainty is the rotation velocity of HI in the SMC (Stanimirovic et al. 2014), which should exceed the amount of rotation in the young stellar component. We fit the TGAS PM data by themselves, or include also the *HST* PM data (K13). The fit results are listed in Table 3.

4. DISCUSSION

The results obtained here are generally consistent with what has been previously reported in the literature, as summarized in K13 and vdMK14.

The TGAS value for the LMC COM PM (Table 2, column (3)) can be compared to the *HST* measurement $(\mu_W, \mu_N) = (-1.910 \pm 0.020, 0.229 \pm 0.047)$ mas yr^{-1}. Similarly, the TGAS value for the SMC COM PM (Table 3) can be compared to the *HST* measurement $(\mu_W, \mu_N) = (-0.772 \pm 0.063, -1.117 \pm 0.061)$ mas yr^{-1}. The results from TGAS and *HST* have similar random errors, and the COM PM measurements agree to within these errors. Given this agreement, it is likely that results of the joint analysis of the *HST* and TGAS data, as reported in Tables 2 and 3, yield the most accurate estimates to date.

The values of the TGAS COM PMs are not strongly dependent on the details of our PM field models. Since the stars are distributed more-or-less symmetrically around the center, a mean of the PM data (Table 1) yields results that are similar to our best fits at the level of the random errors. The exception is the mean μ_W for the LMC, which is affected by the paucity of TGAS stars on the southeast side.

We have not explicitly included possible spatial correlations in TGAS PM errors (Gaia Collaboration et al. 2016b; Lindegren et al. 2016) in our analysis. The

Table 3
SMC Dynamical Model Parameters: Fit Results from Two-Dimensional Kinematics

Quantity	Unit	$V_{\rm rot}$ varied center: HI	$V_{\rm rot}$ varied center: old stars	$V_{\rm rot}$ fixed center: HI	$V_{\rm rot}$ fixed center: old stars
(1)	(2)	(3)	(4)	(5)	(6)
α_0	deg	$16.25 \pm 0.20^{[1]}$	$12.80 \pm 0.20^{[1]}$	$16.25 \pm 0.20^{[1]}$	$12.80 \pm 0.20^{[1]}$
δ_0	deg	$-72.42 \pm 0.20^{[1]}$	$-73.15 \pm 0.20^{[1]}$	$-72.42 \pm 0.20^{[1]}$	$-73.15 \pm 0.20^{[1]}$
PMs TGAS					
μ_{W0}	mas/yr	-0.876 ± 0.060	-0.779 ± 0.052	-0.854 ± 0.105	-0.791 ± 0.060
μ_{N0}	mas/yr	-1.227 ± 0.042	-1.213 ± 0.058	-1.215 ± 0.087	-1.256 ± 0.103
V_0	km/s	-14.3 ± 14.9	-21.7 ± 16.5	$0.0 \pm 40.0^{[1]}$	$0.0 \pm 40.0^{[1]}$
PMs TGAS+HST					
μ_{W0}	mas/yr	-0.742 ± 0.044	-0.723 ± 0.025	-0.777 ± 0.112	-0.720 ± 0.070
μ_{N0}	mas/yr	-1.101 ± 0.045	-1.172 ± 0.044	-1.128 ± 0.099	-1.165 ± 0.106
V_0	km/s	14.0 ± 14.9	3.4 ± 14.3	$0.0 \pm 40.0^{[1]}$	$0.0 \pm 40.0^{[1]}$

Note. — Column (1)-(2): model quantity and units, defined similarly as in Table 2. Columns (3)-(6): values inferred from model fits described in Section 3.
[1] Value kept fixed. Not fit, but uncertainty propagated into other model parameters.

effect of such correlations would be to underestimate the random error in the weighted average PM of a stellar sample (Kroupa & Bastian 1997). We also did not account for the covariances between the astrometric parameters of individual stars, because those are generally small.[2] Our final COM PM errors are dominated by uncertainties in our understanding of the geometry and kinematics of the LMC/SMC, and not by the individual PM measurement errors. Hence, a somewhat approximate treatment suffices. The agreement between our TGAS results and the *HST* results implies that any residual systematics introduced by these approximations must be below the random errors.

We also considered Tycho-2 stars in the TGAS catalog. The Tycho-2 catalog goes fainter, to $V \sim 14$, than the *Hipparcos* catalog, but the typical TGAS PM uncertainty $\gtrsim 1$ mas yr^{-1} is much worse. We selected Tycho-2 stars in the areas of the LMC and SMC, with LOS velocities from the SIMBAD database or the RAVE survey (Kordopatis et al. 2013) that are consistent with LMC or SMC membership. Stars with discrepant PMs were excluded. This yielded 210 LMC and 34 SMC stars, which still includes possible remaining foreground contamination. We found this insufficient to obtain an accurate independent estimate of the LMC and SMC COM PMs.

Joint analysis of TGAS and *HST* PM data well defines the LMC dynamical center (Table 2, column (4)) and yields a result that is consistent with the average dynamical center from HI measurements. For the SMC, the location of the stellar dynamical center is not well known a priori, and it is not well constrained by the PM data. This introduces an additional uncertainty in the COM PM at the level of ~ 0.1 mas yr^{-1} (as evidenced by the results in Table 3 for different assumed centers). This uncertainty is less pronounced when the TGAS and *HST* PM data are analyzed jointly.

The viewing angles (i, Θ) of the LMC disk are not accurately known, with different methods yielding results that differ at the level of tens of degrees. The new results in Table 2 are within the range of what has been found by other studies, but are not sufficiently accurate to convincingly pin down the values of these angles.

The LMC rotation curve inferred from the TGAS data is more useful than that derived from the *HST* PM data, because it pertains to a single stellar population instead of a mixed population. The rotation amplitude for $R \gtrsim 2$ kpc is consistent with that inferred from LOS velocity measurements for young stars (Figure 2), further validating the accuracy of the TGAS data. However, at $R \lesssim 2$ kpc the TGAS-inferred rotation curve lies somewhat below the LOS rotation curve. This could be due to shot noise and the limited number of (ten) TGAS stars at these radii, or it could reflect shortcomings in our kinematical model for the young stellar disk (e.g., warping; Nikolaev et al. 2004).

The LMC PMs are measured in mas/yr, while LOS velocities are measured in km/s. Comparison therefore yields a kinematic estimate of the galaxy distance. The distance modulus implied by a joint fit is $m - M = 18.53 \pm 0.42$ (Table 2, column (5)). This is consistent with the canonical $m - M = 18.50 \pm 0.10$ (Freedman et al. 2001), but not competitive in terms of accuracy. This is due in part to the random errors on the PM rotation curve, and in part to the random errors on the inclination of the disk. But this method for determining the LMC distance will become more competitive with future *Gaia* data releases.

The TGAS data for the SMC do not imply a significant rotation in its young stellar population (see $V_{\rm rot}$ in Table 3), and certainly less than the ~ 40 km s^{-1} rotation amplitude of HI (Stanimirovic et al. 2004). Whether the young SMC stars show more rotation than the old stars, as suggested by LOS velocity data (Evans & Howarth 2008; Harris & Zaritsky 2006), remains unclear.

5. CONCLUSIONS

We have used the *Gaia* DR1 to obtain new insights into the motions and internal kinematics of the MCs. The results do not improve upon the accuracy of existing *HST* studies, but they have similar accuracy and are consistent to within the uncertainties. Since these missions use different methods with different systematics, this provides an external validation of each approach. The TGAS results confirm the large PM of the MCs, which has previously been used to revise our understanding of their

[2] The average correlation between PM_W and PM_N is smaller than 0.1 for the LMC TGAS stars.

orbital history and cosmological context (K13). Both *Gaia* and *HST* (vdMK14) confidently detect and quantify the rotation of the LMC disk using time baselines of a few decades or less, even though it takes the LMC disk in excess of 10^8 years to complete one revolution around its center. Comparison of the LMC rotation curves from PM and LOS data yields a kinematic distance estimate that is independent from, but consistent with, that from photometric methods and the cosmological distance ladder.

The results presented here are the first from the *Gaia* mission on the topic of LG dynamics. *Gaia*'s future data releases will contain many more stars and have higher PM accuracy. With the methods used here, this is guaranteed to further improve our understanding of the MCs. When combined with studies of other nearby targets, this will revolutionize our understanding of the MW and its satellites. For PM studies further out into the LG, and especially for dwarf galaxies with old stellar populations, *HST* will continue to be the telescope of choice due to its ability to measure accurate PMs for faint stars ($V \lesssim 25$) over small fields (e.g., Sohn et al. 2015).

R.v.d.M. is grateful to Nitya Kallivayalil and Gurtina Besla for long-standing collaboration on the proper motion dynamics of the Magellanic Clouds, and to all HSTPROMO members for discussions on these and related topics. J.S. was supported by an ESA Research Fellowship in Space Science. This work has made use of data from the ESA space mission *Gaia* (`http://www.cosmos.esa.int/gaia`), processed by the *Gaia* Data Processing and Analysis Consortium (DPAC, `http://www.cosmos.esa.int/web/gaia/dpac/consortium`). Funding for the DPAC has been provided by national institutions, in particular the institutions participating in the *Gaia* Multilateral Agreement.

Facilities: Gaia.

REFERENCES

Barbier-Brossat, M., Petit, M., & Figon, P., et al. 1994, A&AS, 108, 603
Besla, G., Kallivayalil, N, Hernquist, L., Robertson, B., Cox, T. J., van der Marel, R. P., & Alcock, C. 2007, 668, 949
Besla, G., Kallivayalil, N., Hernquist, L., van der Marel, R. P., Cox, T. J., Keres, D. 2012, MNRAS, 421, 2109
Brunthaler, A., Reid, M. J., Falcke, H., Greenhill, L. J., & Henkel, C. 2005, Science, 307, 1440
Cioni, M.-R. L., Habing, H. J., & Israel, F. P. 2000a, A&A, 358, L9
Cioni, M.-R. L., van der Marel, R. P., Loup, C., & Habing, H. J. 2000b, A&A, 359, 601
ESA 1997, VizieR Online Data Catalog, 1239, 0
Evans, C. J., & Howarth, I. D. 2008, MNRAS, 386, 826
Freedman, W. L., et al. 2001, ApJ, 553, 47
Gaia Collaboration, Prusti, T., de Bruijne, J. H. J., et al., 2016a, The Gaia mission, A&A, in press prep. [http://dx.doi.org/10.1051/0004-6361/201629272]
Gaia Collaboration, Brown, A. G. A., et al. 2016b, A&A, in press [http://dx.doi.org/10.1051/0004-6361/201629512]
Harris, J., & Zaritsky, D. 2006, AJ, 131, 2514
Kallivayalil, N., van der Marel, R. P., Alcock, C., Axelrod, T., Cook, K. H., Drake, A. J., & Geha, M. 2006a, ApJ, 638, 772
Kallivayalil, N., van der Marel, R. P., & Alcock, C. 2006b, ApJ, 652, 1213
Kallivayalil, N., van der Marel, R. P., Besla, G., Anderson, J., & Alcock, C. 2013, ApJ, 764, 161 (K13)
Kordopatis, G., et al. 2013, AJ, 146, 134
Kroupa, P., & Bastian, U. 1997, New Astronomy, 2, 77
Lindegren, L., Lammers, I., Bastian, U., Hernandez, J., Klioner, S., Hobbs, D., Bombrun, A., & Michalik, D. 2016, A&A, in press [http://dx.doi.org/10.1051/0004-6361/201628714]
Neugent, K. F., Massey, P., Skiff, B., & Meynet, G. 2012, ApJ, 749, 177
Nikolaev, S., Drake, A.J., Keller, S. C., Cook, K. H., Dalal, N., Griest, K., Welch, D. L., & Kanbur, S. M. 2004, 601, 260
Sohn, S. T., van der Marel, R. P., Carlin, J. L., et al. 2015, ApJ, 803, 56
Stanimirovic, S., Staveley-Smith, L., & Jones, P. A. 2004, ApJ, 604, 176
van der Marel, R. P. 2015, in "Galaxy Masses as Constraints of Formation Models," Proc. IAU, Vol. 311, p. 1
van der Marel, R. P., Alves, D. R., Hardy, E., & Suntzeff, N. B. 2002, AJ, 124, 2639 (vdM02)
van der Marel, R. P., Kallivayalil, N., & Besla, G. 2009, in "The Magellanic System: Stars, Gas, and Galaxies," Proc. IAU Symposium 256, 81
van der Marel, R. P., & Kallivayalil, N. 2014, ApJ, 781, 121 (vdMK14)